

## 3D femoral neck anteversion measurements based on the posterior femoral plane in ORTHODOC<sup>®</sup> system

Yeon Soo Lee · Seung Hoon Oh · Jong Keun Seon · Eun Kyoo Song · Taek Rim Yoon

Received: 15 September 2005 / Accepted: 21 August 2006 / Published online: 29 September 2006  
© International Federation for Medical and Biological Engineering 2006

**Abstract** This study provides a robust measuring method of the femoral neck anteversion angle for use in a total hip replacement pre-planning program. The femora of 24 patients ( $69.3 \pm 6.3$  years old) were CT-scanned and converted into three-dimensionally volume-rendered models in ORTHODOC<sup>®</sup> (ISS Inc., CA, USA) which is the pre-planning software for ROBODOC surgery. The Mod.ISS method (the modified ISS method), designed by authors, measures the anteversion angle of the proximal-most femoral neck confluence on the plane perpendicular to the femoral mechanical axis. 3D FNC method proposed by the authors of the present study involves measurement of the anteversion angle of three-dimensional femoral neck center on a plane perpendicular to the posterior femoral plane and parallel to the posterior condylar axis. Here, we found that inte-

robserver reproducibility was  $1.8^\circ$  (SD = 1.3) for the Mod.ISS method and  $2.4^\circ$  (SD = 1.9) for the proposed 3D FNC method. The anteversion angle of the local femoral neck axis was measured as  $\theta = 25.3(L/D) - 5.4$  in  $L/D = 0.1 \sim 0.6$ , where  $L/D$  is distance ( $L$ ) from the proximal-most neck confluence along the femoral mechanical axis, normalized with respect to the diameter of the femoral head ( $D$ ). At  $L/D = 0.5$ , the anteversion angle of the femoral neck axis was coincident with the average femoral neck anteversion determined by the 3D FNC method. We conclude that the 3D FNC method is a gold standard for measuring the femoral neck anteversion applicable during both pre-operative and post-operative stages, because its femoral neck center can be determined in three-dimensional space during both stages.

Y. S. Lee  
Department of Information and Mechatronics Engineering,  
GwangJu Institute of Science and Technology,  
GwanJu, Republic of Korea  
e-mail: biomechanics.yslee@gmail.com; yeonslee@gist.ac.kr

J. K. Seon · E. K. Song · T. R. Yoon  
Center for Joint Disease,  
Chonnam National University Hwasun Hospital,  
Ilsimli 160, Hwasungun, Jeollanamdo 519-809,  
Republic of Korea

E. K. Song · T. R. Yoon ✉  
Department of Orthopaedic Surgery, Medical School,  
Chonnam National University, GwangJu 519-809,  
Republic of Korea  
e-mail: tryoon@chonnam.ac.kr

S. H. Oh  
Rocom Frontier Co Ltd,  
Seoul, Republic of Korea

**Keywords** Femoral neck anteversion · ORTHODOC · ROBODOC · Hip · Pre-planning

### 1 Introduction

Using computer preplanning systems for robot-assisted orthopedic surgery, measurements of three-dimensional (3D) femoral neck anteversion are applicable in the real clinical environment. The clinical function of femoral neck anteversion is well documented by the fact that it affects in- or out-toeing, dislocation, range of motion, soft tissue strain [3], bone mineral density and bone shape [2], femoral stress [19], contact force [5], and osteolysis [18]. Moreover, increased femoral neck anteversion may introduce in-toeing, and increase hip lateral rotation and congenital hip dislocation, while reduced femoral neck anteversion may cause

tearing of the acetabular labrum of the hip and out-toeing [3]. It has been reported that increase of femoral anteversion is associated with a significant elevation in the bone mineral density of femoral neck bone and trochanter [2]. Moreover, a significant correlation was found between the extent of neck version and compressive strain on the side toward which the prosthetic neck was oriented [19]. In addition, increasing the femoral neck anteversion to an angle of 30° increased hip contact forces and bending moments up to 28% [6], whereas increasing femoral neck anteversion with total hip replacement (THR) femoral component was associated with a reduction in the posterior dislocation of the femoral head and increased stability [5]. On the other hand, reduced femoral neck anteversion may produce a deformity that results in osteoarthritis independently of other deformities [18]. This established that femoral neck anteversion angles (FNAA) should be correctly measured pre-operatively and be considered during the pre-planning of THR surgery.

Femoral neck anteversion angles in existing literature range from 0 to 40°, which demonstrates a huge standard deviation and differences between races and observers [1, 7, 12, 14, 16]. Large discrepancies and variations in FNAA may be due to different definitions of femoral neck anteversion, inaccurate measurement tools, and the positioning of specimens. Angle measurements using biplane radiography and monoplane radiography are neither accurate nor repeatable [9, 10, 12, 17], and those based on two-dimensional (2D) CT images have the same problems [12, 15]. For living patients, only 3D angle measurement using 3D models can provide a robust measurement method, because the skeletal alignments of patients achieved by CT based model can be reproducible. Computer preplanning systems for robot-assisted orthopedic surgery are designed to measure true 3D angles. However, no method has been established as a gold standard to measure the femoral neck anteversion for the pre-planning of robot-assisted THR surgery.

Most methods used to measure 3D femoral neck angle fall far short of practical application in living patients. From the late 1990s, measurements of true 3D femoral neck anteversion were proposed by several researchers [4, 8–10, 13–10, 17]. To minimize the human factor, several studies used complex numerical process to decide upon a principal axis using multi-layer edge contours [10, 13, 17]. However, even complex calculations supported by additional numerical processing may not guarantee accuracy [9, 10] and also their complexities make their methods difficult to be used in the clinical environment. Thus, a robust and

easily used 3D femoral neck anteversion measurement protocol should be devised for use in the clinical environment.

To this end, we propose a robust and repeatable measurement method of femoral neck anteversion based on the ORTHODOC<sup>®</sup> preplanning program for the ROBODOC<sup>®</sup> orthopedic surgery system [Integrated Surgical Systems (ISS), CA, USA]. The proposed method involves adaptations of the methods described by Kim et al. [9], and Kingsley and Olmsted's [11] in terms of defining the femoral neck axis (FNA) and the posterior femoral plane (PFP) including the posterior condylar axis (PCA), respectively. For comparative purposes, we include the modified ISS method devised by current authors that measures the anteversion of the proximal-most femoral neck confluence.

## 2 Materials and methods

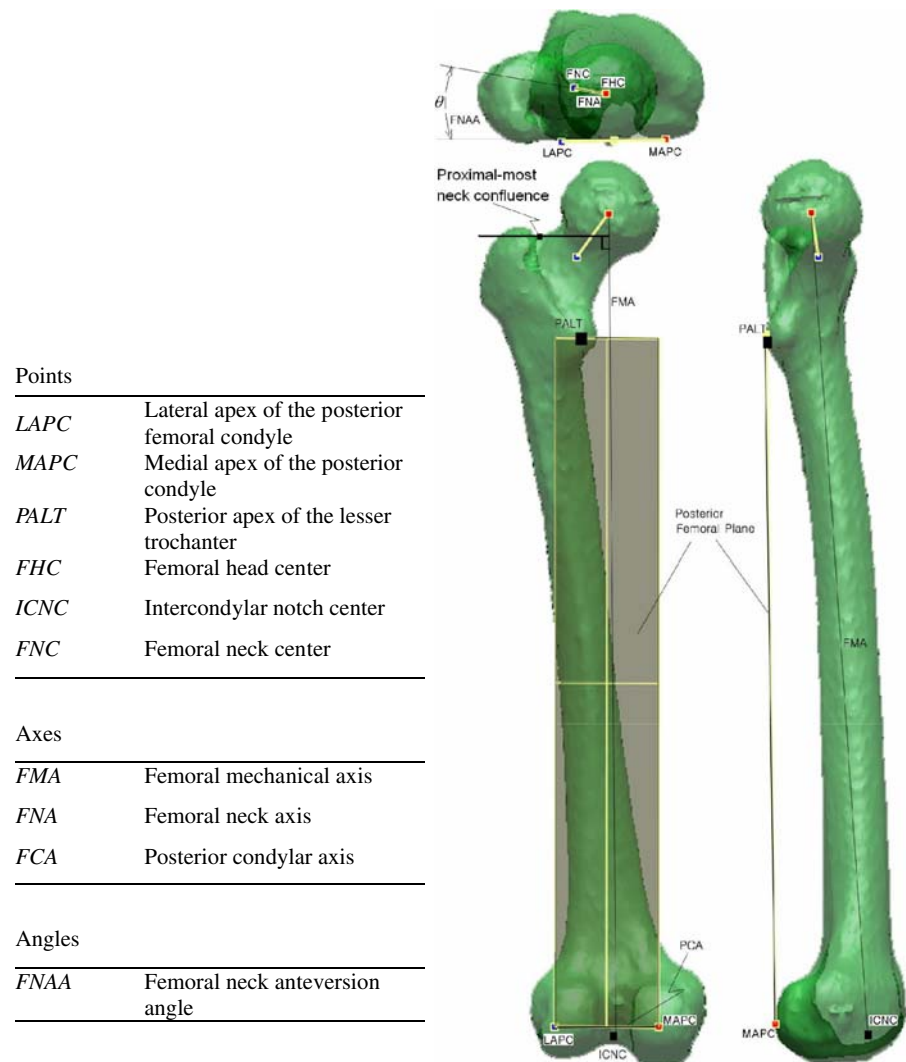
Measurements of femoral neck anteversion depend on three key geometric axes, i.e., the femoral shaft alignment axis, the PCA, and the FNA [9]. ISS (Integrated Surgical Systems, CA, USA) has used its own method, i.e., the ISS method that involves measuring the anteversion of the proximal-most femoral neck confluence relative to the PCA of the femur. To determine femoral neck anteversion using this ISS method, the proximal-most femoral neck confluence and the posterior condylar apexes of the femur are overlapped on proximal-to-distal plane view. However, this view is dependent on observer's choice, and thus the ISS method inevitably has poor intra and interobserver repeatability. To improve these repeatability, the authors modified the ISS method such that the proximal-to-distal plane view is displayed perpendicular to the femoral mechanical axis (FMA) [20]. We refer to this modified ISS method as Mod.ISS.

In addition, the 3D femoral neck center (3D FNC) method, proposed by the authors at current study, measures the FNAA on a simulated PFP [11]. The 3D FNC method and the Mod.ISS method are explained in detail in section II.2. The authors recommend that the reader refers Fig. 1 before proceeding as it defines the abbreviations used in this manuscript.

### 2.1 3D femur models and the ORTHODOC<sup>®</sup> system

Twelve left and 12 right knees (from 24 Korean females of mean age  $69.3 \pm 6.3$  years) were scanned by

**Fig. 1** Abbreviation used in current study



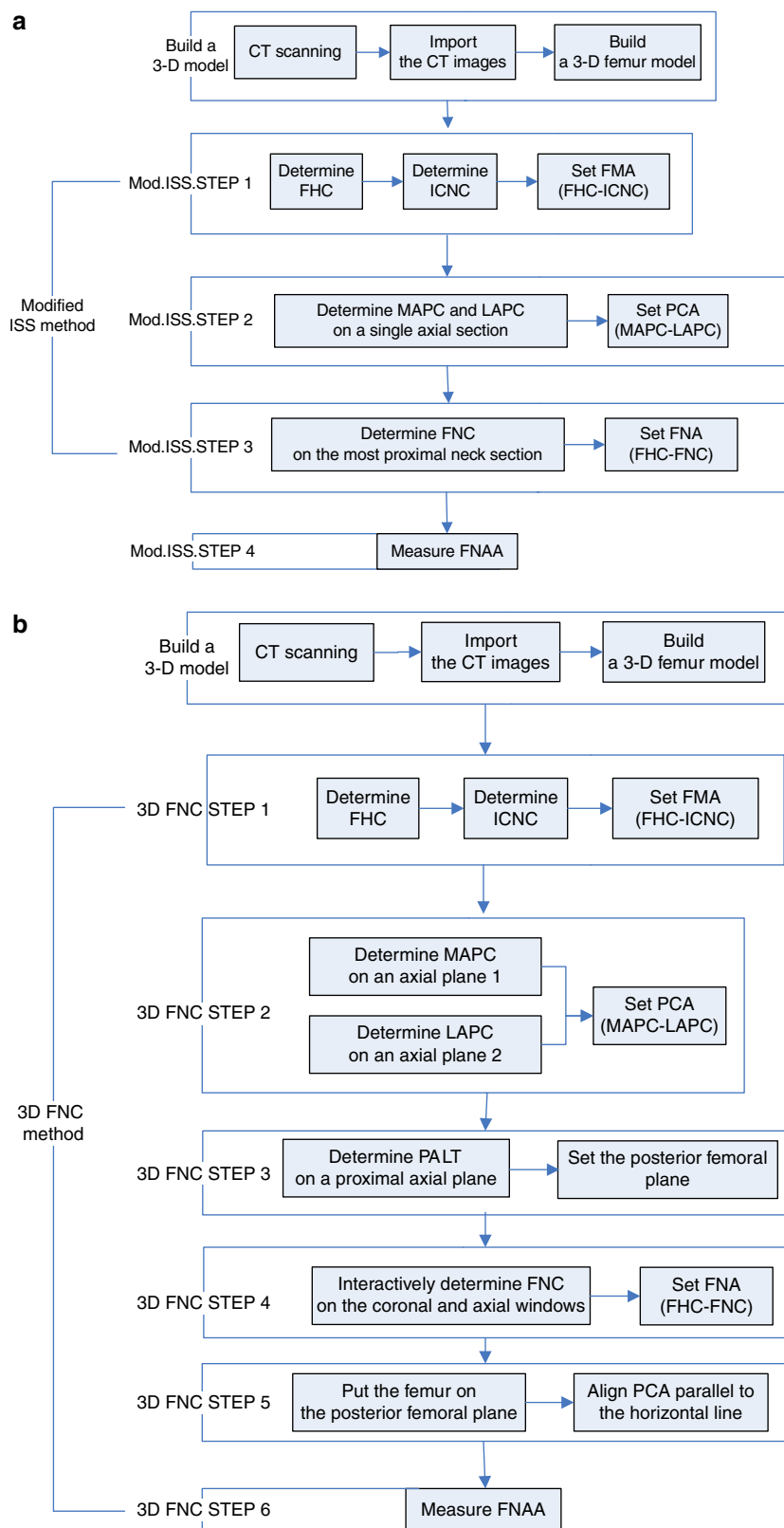
computer tomography (CT). The CT images were scanned at a slice thickness of 1.25 mm and then imported into ORTHODOC®. These imported 2D CT images were then converted into volume rendered 3D bone models of gray value 80, as scaled by ORTHODOC®'s proprietary conversion of Hounsfield Units. ORTHODOC® displays four windows including three orthogonal section windows, namely, sagittal, coronal, and axial windows, and one isotropic window. Anatomical reference points can be registered in a 3D bone model. ORTHODOC® has a function that enables geometric features such as points and axes to be registered onto a 3D model space. Once geometric features, such as femoral head center (FHC) or a femoral PCA, have been unequivocally registered, these registered features are maintained in their unique anatomic positions in 3D model space.

## 2.2 Measurement of femoral neck anteversion angle

### 2.2.1 Modified ISS method

During THR pre-planning using ORTHODOC®, the alignment of the femoral stem is determined by referring to the FHC, the proximal femoral intramedullary canal, and the posterior femoral condyles. The FNAA is measured on an axial plane perpendicular to the femoral longitudinal axis. The original ISS method, has been adopted by Integrated Surgical Systems (ISS, CA, USA), measures the FNAA on axial planes perpendicular to the proximal intramedullary canal axis, along which the femoral stem will be inserted. However, the determination of the proximal intramedullary canal axis is somewhat subjective in that the longitudinal path of the intramedullary canal is not straight and the direction

**Fig. 2** The work flows of the modified ISS method (Mod.ISS method) and the three-dimensional femoral neck method (3D FNC method) for femoral neck anteversion angle (FNAA). **a** The measurement flow of the FNAA by the ISS method. **b** The measurement flow of the FNAA by the 3D FNC method



of the canal axis changes from proximal to distal. These ambiguous characteristics concerning the determination of the proximal intramedullary canal axis inevitably

produce poor intra and interobserver repeatability in terms of getting the longitudinal axial images perpendicular to the intramedullary canal axis. To obtain

anatomically standardized axial images independent on patient position at CT scanning, it is necessary to set a standardized longitudinal axis perpendicular to the direction in which axial images will be built.

The authors constructed a modification of the ISS method (Mod.ISS) by adopting the FMA rather than the proximal intramedullary canal axis. Mod.ISS involves measuring the FNAA on axial images perpendicular to the FMA. A schematic of the method use to determine FNAA using Mod.ISS is described in four steps (Fig. 2a).

### 2.3 Mod.ISS.STEP 1 Determination of the femoral mechanical axis

To obtain anatomically standardized patient position at the stage of CT-scanning, the authors adopted the FMA. The FMA of a 3D femoral model was aligned parallel to the vertical direction of the coronal window. The position of FHC was determined by placing a circle onto the circumference of the femoral head on a set of three orthogonal section views, (i.e., axial, coronal, and sagittal views) showing the largest bone contour of the femoral head. The FHC locations were determined as the center of the circle that best matched largest bone contours (Fig. 3a-i). The intercondylar notch center (ICNC) was defined as the middle of the line connecting the narrowest anterior-to-posterior borders on an axial section of the distal femur. The position of ICNC varies in the axial direction, and the volume-rendered 3D model does not provide a clear bone contour when the closest distance between anterior-posterior borders is less than 5 mm. Hence, ICNC location should be determined using an axial image on which the anterior and posterior borders of the intercondylar notch are shown clear. In the present study, an axial image with an anterior-posterior width of 10 mm was considered proper in terms of defining ICNC position, because it allowed a relatively clear bone contour to be observed in the corresponding axial view. ICNC position was determined by placing a circle of 10 mm diameter on axial images with an anterior-posterior width of 10 mm (Fig. 3a-ii). The FMA was defined as the line passing through the FHC and the ICNC [20], and FMA were aligned parallel to the vertical axes of the coronal and sagittal windows (Fig. 3a-iii).

### 2.4 Mod.ISS.STEP 2 Determination of the posterior condylar axis

The medial apex of the posterior condyle (MAPC) and the lateral apex of the posterior condyle (LAPC) are located in a single axial plane including the posterior-

most medial condyle, perpendicular to the FMA (Fig. 3b). The PCA was defined as the line connecting MAPC and LAPC.

### 2.5 Mod.ISS.STEP 3 Determination of the femoral neck axis

Femoral neck axis was drawn using proximal-most neck confluence and FNC. FNC is the proximal-most neck intersection of extensions of the greater trochanter and the femoral head (Fig. 3c). FNA was defined as a line connecting the FHC and femoral neck center (FNC).

### 2.6 Mod.ISS.STEP 4 Measurement of the femoral neck anteversion angle

The FNAA was measured on the axial plane including the medial and lateral apices of the posterior condyle (MAPC and LAPC). The Mod.ISS method defines the FNAA as the angle included between the FNA and the PCA on the axial plane perpendicular to the FMA (Fig. 3d).

#### 2.6.1 3D FNC method

The 3D FNC method determines the FNC by finding the 3D center point of the narrowest part of the femoral neck as described by Kim et al. [9], and measures the FNAA referred to the simulated PFP of Kingsley and Olmsted's [11] that includes the medial and lateral apices of the posterior condyle and the most prominent posterior point of the lesser trochanter. A schematic of the determination of FNAA using the 3D FNC method is shown in Fig. 2b, and the detail of the process required to determine anatomical points and axes is explained in Fig. 4.

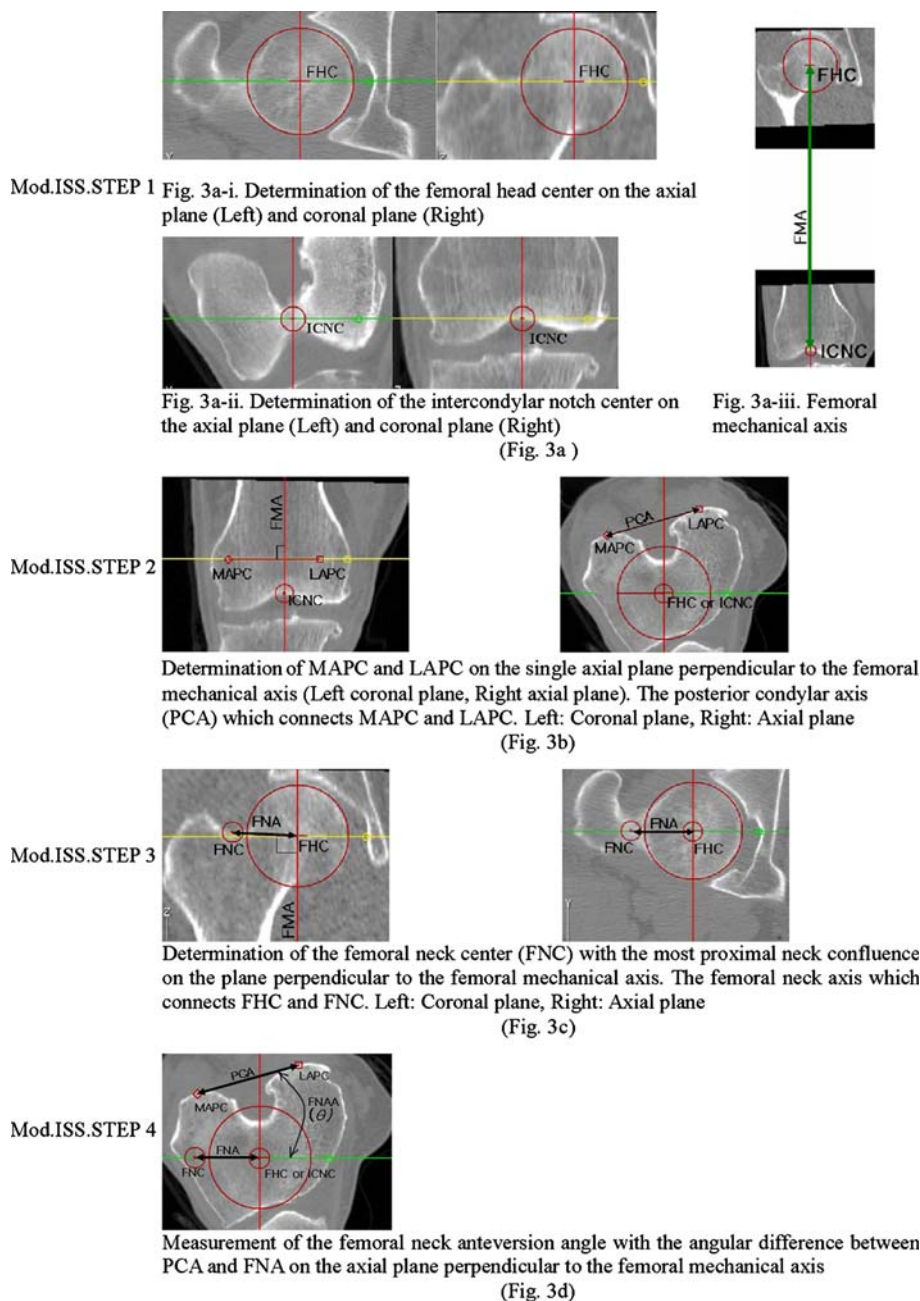
### 2.7 3D FNC STEP 1 Determination of the femoral mechanical axis

The FHC, ICNC, and FMA were determined as described in Mod.ISS.STEP 1 (Fig. 4a).

### 2.8 3D FNC STEP 2 Determination of the posterior condylar axis

The PCA was determined whilst keeping FMA aligned parallel to the vertical lines of the coronal and sagittal windows. The medial and lateral apices of the posterior condyles (MAPC and LAPC) were determined by separately finding each posterior-most point. Initially, the medial apex of the posterior femoral condyle

**Fig. 3** The measurement of FNAA by the Mod.ISS method. The ISS preferred method that measures the anteversion of the proximal-most femoral neck confluence relative to the posterior condylar axis of the femur on the proximal-to-distal plane perpendicular to the femoral mechanical axis



(MAPC) was determined on the axial window that includes the posterior-most prominence of the medial posterior condyle. Second, the lateral apex of the posterior femoral condyle (LAPC) was determined in the same manner as described above for determining MAPC. The PCA was then built by connecting the MAPC and LAPC (Fig. 4b).

2.9 3D FNC STEP 3 Determination of the posterior apex of the lesser trochanter

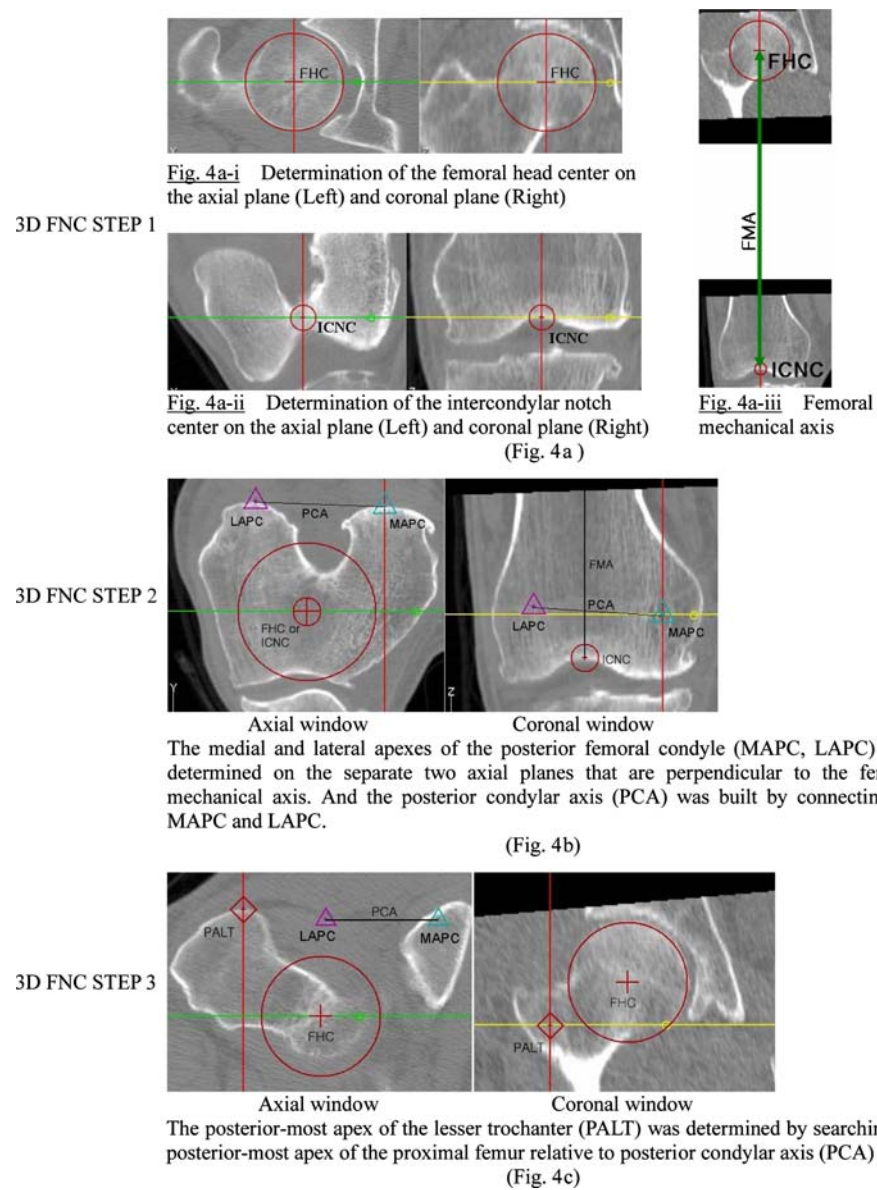
The posterior apex of the lesser trochanter (PALT) was determined in the plane perpendicular to the

FMA. MAPC, LAPC, and PALT are the three points required to construct the PFP. PALT was determined by locating the posterior-most apex of the lesser trochanter relative to the PCA (Fig. 4c).

2.10 3D FNC STEP 4 Determination of the femoral neck axis

The FNA was built by connecting the FHC and the FNC. FNC was determined in 3D space by considering its position on axial and coronal planes (Fig. 4d). First, the narrowest neck portion was searched for in the coronal plane by placing a circle

**Fig. 4** The measurement of FNAA by the 3D FNC method. The 3D FNC method measures the anteversion angle of the three-dimensional femoral neck axis referred to the simulated posterior femoral plane of Kingsley and Olmsted's [11] that includes the medial and lateral apices of the posterior condyle and the most prominent posterior point of the lesser trochanter. The femoral neck center (FNC) is determined as the three-dimensionally narrowest FNC which is determined as the center point of the narrowest part of the femoral neck as described in Kim et al's study [9]



on the contour of the narrowest neck portion. Second, in the axial plane, the circle was again placed on the contour of the narrowest neck portion. This determination process for FNC was repeated until the center of these circles did not change its position. The final position of the center of the circle was determined as the FNC.

**2.11 3D FNC STEP 5 Placement of the femur on the posterior femoral plane**

The PFP was located using three reference points, i.e., the medial apices of the posterior condyle (MAPC and LAPC), and the PALT. The femur model was placed on the PFP, and the PALT–MAPC line and the PCA of the femur model were aligned to the vertical line

and to the horizontal line of the coronal window, respectively, and sequentially (Fig. 4e).

**2.12 3D FNC STEP 6 Measurement of the femoral neck anteversion angle**

The FNAA was measured on the axial plane parallel to the PCA and perpendicular to the PFP, and was defined as the angle included between the PCA and the FNA (Fig. 4f).

**2.13 Anteversion angle of the local femoral neck axis**

After measuring the FNAA using the 3D FNC method, anteversion of the FNA was measured locally on

Fig. 4 continued

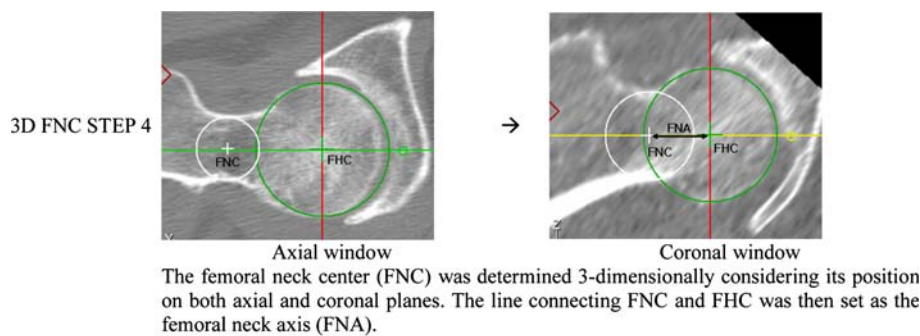


(Fig. 4d)

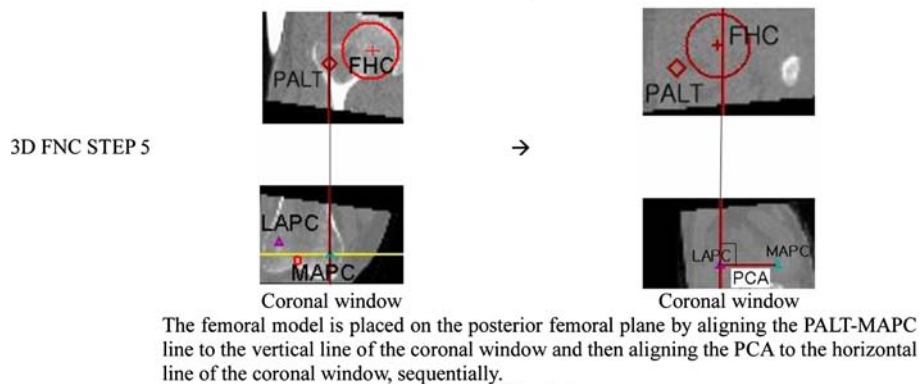


(Fig. 4e)

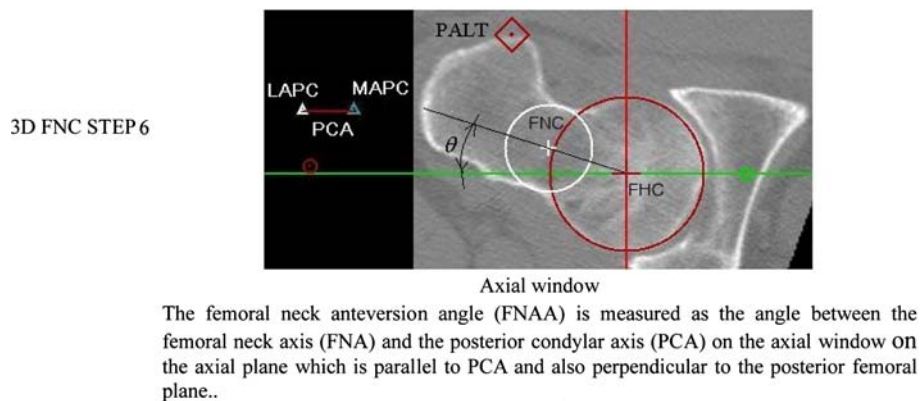


(Fig. 4f)

axial planes perpendicular to the FMA. This anteversion angle of the local FNA was measured distally in 5 mm increments from the proximal-most neck confluence, i.e., the intersection of the greater trochanter and the femoral head. To anatomically and parametrically assess the variance in the anteversion angle of the local FNA, the distal distance ( $L$ ) from the proximal-most neck confluence was normalized with the diameter of the femoral head ( $D$ ) (Fig. 6b). The normalized distal distance ( $L/D$ ) starts from the proximal-most neck confluence and advances along the FMA (Fig. 5). The local FNC was defined as the center of the narrowest neck portion on each axial image, and the local FNA was defined as the line connecting the

and the local FNC. Then, the anteversion of the local FNA was measured as the angular difference between the local FNA and the PCA in the axial window, which lies perpendicular to PCA.

## 2.14 Statistical analysis

Intraobserver measurement error was determined from difference between the first and second measurements of a single observer. Interobserver reproducibility of the each method was determined by calculating the standard deviation of the difference between the values measured by two observers for each method. Statistical analysis was performed using



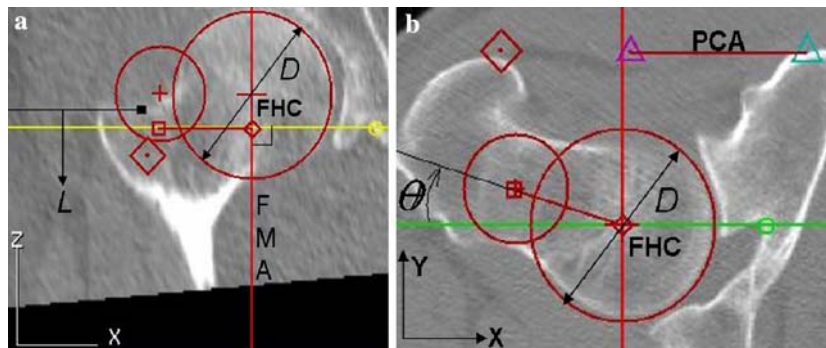


**Fig. 5** Geometric expression to measure the anteversion angle of local femoral neck axis. **a** Demonstrates the normalized distal distance ( $L/D$ ) from the proximal-most neck confluence. The  $L$  is the distance from the most proximal neck confluence along the femoral mechanical axis and  $D$  is the diameter of the femoral head. **b** Shows that the anteversion angle of the femoral neck axis was locally measured on the axial view. The local FNC was

defined as the center of the narrowest neck portion on each axial image. The local femoral neck axis (local FNA) was defined as the line connecting the femoral head center (FHC) and the local FNC. Then, the anteversion angle of the local FNA was measured as the angular difference between the local FNA and the posterior condylar axis (PCA) in the axial window, which lies perpendicular to PCA

univariate repeated measures ANOVA with the Turkey post hoc test. The level of significance ( $P$ ) was set as 0.05.

### 3 Results

The FNAA measured by two observers averaged  $8.6^\circ$  ( $SD = 7.0^\circ$ ) for the Mod.ISS method and  $18.5^\circ$  ( $SD = 7.2^\circ$ ) for the 3D FNC method. Interobserver error was  $1.8^\circ$  ( $SD = 1.3^\circ$ ) for the ISS method and  $2.4^\circ$  ( $SD = 1.9^\circ$ ) for the 3D FNC method (Table 1; Fig. 6a).

No statistical difference in measurement repeatability was observed between the two methods, and both showed a small repeatability error at  $1^\circ$  for interobserver and intraobserver repeatabilities (Fig. 6a, b). When measuring the FNAA using the Mod.ISS method, the intraobserver measurement error was  $0.6^\circ$  ( $SD = 0.5^\circ$ ) for observer 1 and  $0.9^\circ$  ( $SD = 0.6^\circ$ ) for observer 2, and when measuring FNAA using the 3D FNC method, the intraobserver measurement error

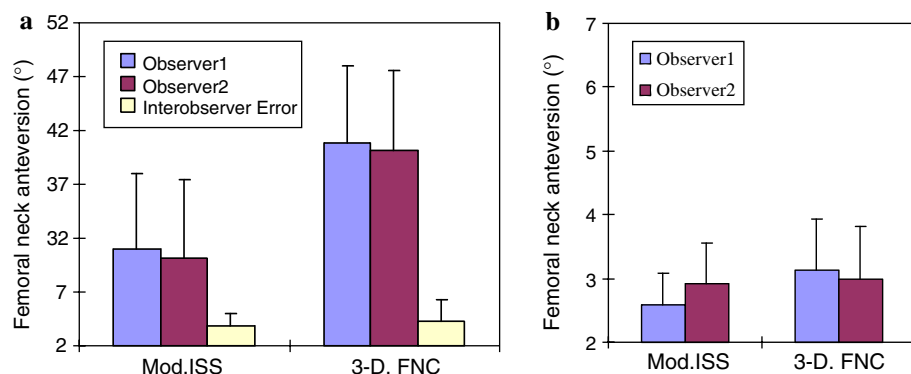
was  $1.1^\circ$  ( $SD = 0.8^\circ$ ) for observer 1 and  $1.0^\circ$  ( $SD = 0.8^\circ$ ) for observer 2 (Fig. 6b).

The anteversion angle of the local FNA varied little until the  $L/D$  ratio reached  $=0.1$ . However in the  $L/D$  ratio range of  $0.1 \sim 0.6$ , the anteversion angle of the local FNA increased linearly proportional to the distal distance (Fig. 7). The variance in the anteversion angle of the FNA can be expressed as a function of the normalized distance ( $L/D$ ) from the proximal-most neck confluence on the axial plane. The equation used to present the anteversion angle of the local FNA was as follows;

$$\theta^\circ = 25.3(L/D) - 5.4 \text{ in } L/D = 0.1 \sim 0.6 \quad (1)$$

In Fig. 7, the femoral neck anteversion angle (FNAA) by the Mod.ISS method was close to the local FNAA within  $L/D = 0 \sim 0.1$  while FNAA by the 3D FNC method coincided at  $L/D = 0.5$ . The diameter of the femoral head ( $D$ ) came to an average of  $42.8 \text{ mm}$  ( $SD = 1.8$ ).

**Fig. 6** The measured FNAA by the ISS method and the 3D FNC method. **a** Shows the interobserver measurement error was expressed. **b** Shows the intraobserver measurement error for those two methods. Error bars on **a** and **b** are represented by the standard deviation



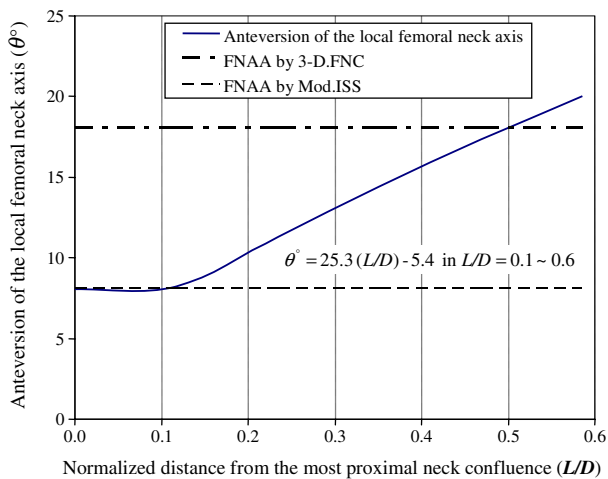


**Fig. 7** The anteversion angle of the local FNA along the femoral mechanical axis. At  $L/D = 0.5$ , the anteversion angle of the local FNA meets the FNAA determined by the 3D FNC method. The anteversion angle of the local FNA is expressed as  $\theta^\circ = 25.3(L/D) - 5.4$  in  $L/D = 0.1 \sim 0.6$

#### 4 Discussion

From the first use of the ORTHODOC<sup>®</sup> pre-planning system for THR surgery using ROBODOC<sup>®</sup>, the authors recognized that it is necessary to establish a new robust means of measuring the FNAA as an alternative to the ISS method. The ISS method originally preferred by ISS has ambiguities concerning the locations of the anatomical landmarks on axial slices normal to the intramedullary axis, along which the femoral stem is placed. Alternatively, when the FNAA is measured using original CT slices, confounding factors such as patient positioning, variable technician skills and radiographic interpretation by clinicians could lead to serious measurement errors [12, 15]. The devised Mod.ISS method provides an advantage over the ISS method in terms of standardization of the measurement plane, which lies perpendicular to the FMA. The Mod.ISS method determines the location of the FMA using a robust protocol that uses identifiable landmarks of the FHC and the ICNC.

In the current study, we evaluated two repeatable methods for measuring the FNAA. The Mod.ISS method and 3D FNC method differ in three ways in which they determine the FNAA. The first difference is the measurement plane. The Mod.ISS method measures FNAA in an axial plane that lies perpendicular to the FMA and parallel to the PCA, whereas the 3D FNC method measures FNAA in an axial plane perpendicular to the PFP and parallel to the PCA. The second difference is how the medial and lateral apexes of the posterior condyle are determined. The Mod.ISS

method determines the lateral apex and the medial apex on a single axial sectional plane that includes the largest MAPC. The 3D FNC method determines the MAPC in one axial plane, which includes the posterior-most MAPC, and the LAPC on another plane, which includes the posterior-most LAPC. The third difference is the way in which the FNC is determined. The Mod.ISS method determines the FNC using the proximal-most neck confluence, whereas the 3D FNC method uses the 3D volumetric center of the narrowest neck portion. The effect of whether the medial and lateral apexes of the posterior condyle (MAPC and LAPC) is determined in a single axial plane or on two axial planes can be interpreted by difference in the FNAA determined using the Mod.ISS method and the local FNAA at  $L0/D$ , (i.e.,  $L/D = 0$ ) (Table 1). That is, once the axial window of the femur has been aligned perpendicular to the mechanical axis, the way to determine the PCA did not affect the FNAA as less as  $0.1^\circ$  ( $SD = 1.6^\circ$ ).

When measuring the 3D FNAA, main error sources emanate from the determinations of three key geometric features, namely: (1) the femoral posterior-most condylar axis; (2) the FNA; (3) the femoral shaft axis [9]. Of these, the first and most prominent source of error comes from the determination of the FNA [7, 9, 15]. The 3D FNC method proposed by the authors uses three technical treatments to reduce errors emanating from the determination process of the three key geometric features. First, the apexes of the femoral posterior condyles were determined by globally finding medial and lateral apexes on separate section images arrayed along the FMA. Second, the FNC was determined by graphically finding the 3D center of the narrowest femoral neck, in a manner similar to that described by Kim et al. [9]. Third, to secure a reproducible specimen position for measuring the FNAA, a 3D computer model of the femur was placed on a simulated PFP [11] and the FMA was aligned perpendicular to the PCA.

The 3D FNC and Mod.ISS methods were both found to be reproducible. Due to the anatomically determined landmarks and femoral alignment utilizing the mechanical femoral axis, both methods can use standardized images, which are independent of the patient position during CT scanning. Even though both methods provide good repeatability, especially the 3D FNC method provides important meanings in terms of clinical applications and biomechanics. Since the proximal-most neck confluence locates posterior in an intact femur, the Mod.ISS method cannot find the posteriorly located proximal neck confluence after THR. In contrast to the Mod.ISS method, the 3D FNC

**Table 1** The femoral neck anteversion angle measured by the Mod.ISS method, the 3D FNC method, and locally measured along the femoral mechanical axis

| Subjects |     |     | FNAA (°) by Mod.ISS (Trial 1 + Trial 2)/2 |      | FNAA (°) by 3D FNC (Trial 1 + Trial 2)/2 |      | FNAA (°) locally along FMA |      |      |      |      |      |
|----------|-----|-----|---|------|--|------|----------------------------|------|------|------|------|------|
| #        | L/R | Age | Observer                                  |      | Observer                                 |      | L/D (observer 2)           |      |      |      |      |      |
|          |     |     | 1   | 2    | 1  | 2    | L0/D                       | L1/D | L2/D | L3/D | L4/D | L5/D |
| 1        | L   | 62  | 5.5                                       | 7.1  | 16.9                                     | 18.7 | 19.0                       | 20.4 | 24.3 | 26.8 | 30.4 | 33.8 |
| 5        | L   | 64  | 14.0                                      | 13.6 | 21.6                                     | 19.7 | 1.9                        | 0.4  | 4.3  | 8.6  | 11.7 | 13.3 |
| 3        | L   | 64  | 6.7                                       | 2.7  | 16.1                                     | 7.8  | 11.9                       | 9.3  | 12.5 | 16.3 | 19.7 | 26.2 |
| 4        | L   | 66  | 1.3                                       | 1.1  | 8.3                                      | 9.1  | 19.2                       | 19.0 | 24.4 | 26.6 | 31.1 | 34.7 |
| 5        | L   | 66  | 4.2                                       | 1.4  | 16.8                                     | 17.6 | -5.8                       | -2.9 | 2.9  | 6.9  | 7.9  | 7.7  |
| 6        | L   | 70  | 19.0                                      | 17.8 | 29.1                                     | 29.3 | 10.3                       | 11.5 | 12.8 | 15.9 | 19.9 | 19.9 |
| 7        | L   | 74  | 4.1                                       | -0.5 | 8.8                                      | 11.3 | 9.0                        | 9.2  | 10.9 | 14.5 | 17.0 | 17.4 |
| 8        | L   | 77  | 7.3                                       | 4.5  | 17.6                                     | 14.5 | 10.3                       | 12.1 | 12.1 | 15.8 | 18.4 | 20.9 |
| 9        | L   | 78  | 7.7                                       | 9.1  | 15.6                                     | 11.7 | 11.5                       | 9.6  | 13.8 | 16.2 | 19.7 | 21.7 |
| 10       | L   | 79  | -8.5                                      | -6.3 | 4.4                                      | 5.8  | 9.4                        | 11.6 | 15.9 | 20.3 | 22.0 | 27.1 |
| 11       | L   | 79  | 12.6                                      | 10.9 | 27.3                                     | 23.3 | 10.2                       | 13.9 | 15.5 | 19.0 | 22.7 | 26.6 |
| 12       | L   | 79  | -0.7                                      | -3.1 | 6.8                                      | 5.2  | 0.0                        | -0.9 | 1.2  | 4.5  | 9.0  | 9.0  |
| 13       | R   | 59  | 19.8                                      | 22.4 | 29.0                                     | 27.8 | 1.3                        | -1.3 | -2.4 | 0.0  | 3.8  | 5.7  |
| 14       | R   | 59  | 13.4                                      | 12.0 | 24.6                                     | 25   | 10.4                       | 8.4  | 11.6 | 11.6 | 14.2 | 14.2 |
| 15       | R   | 64  | 2.3                                       | 2.4  | 12.1                                     | 9.6  | 0.9                        | 0.4  | 6.4  | 8.5  | 9.7  | 13.1 |
| 16       | R   | 64  | 9.0                                       | 10.2 | 16.7                                     | 22   | 1.9                        | 3.9  | 10.5 | 11.1 | 15.1 | 16.6 |
| 17       | R   | 67  | 9.4                                       | 10.4 | 21.3                                     | 20.9 | 14.0                       | 14.5 | 16.7 | 19.5 | 22.1 | 26.0 |
| 18       | R   | 68  | 10.3                                      | 9.0  | 18.1                                     | 18.9 | 8.3                        | 5.1  | 6.8  | 13.1 | 16.7 | 19.8 |
| 19       | R   | 68  | 10.0                                      | 5.9  | 19.5                                     | 16.7 | 14.6                       | 14.6 | 15.5 | 18.4 | 21.3 | 24.3 |
| 20       | R   | 68  | 10.4                                      | 9.8  | 20.4                                     | 20.1 | 18.7                       | 20.0 | 22.1 | 24.0 | 26.7 | 29.6 |
| 21       | R   | 69  | 15.5                                      | 14.6 | 24.5                                     | 22.7 | 5.1                        | 3.9  | 6.4  | 10.1 | 12.0 | 17.0 |
| 22       | R   | 70  | 22.5                                      | 23.2 | 31.0                                     | 29.1 | -4.3                       | -1.6 | 3.7  | 5.3  | 6.4  | 11.1 |
| 23       | R   | 72  | 10.0                                      | 8.8  | 21.0                                     | 17.6 | 6.2                        | 6.5  | 10.7 | 12.9 | 17.0 | 19.7 |
| 24       | R   | 76  | 11.8                                      | 8.7  | 24.8                                     | 30.1 | 9.5                        | 10.0 | 13.0 | 20.7 | 22.0 | 25.7 |
| Average  |     | 69  | 9.0                                       | 8.1  | 18.8                                     | 18.1 | 8.1                        | 8.2  | 11.3 | 14.4 | 17.4 | 20.0 |
| SD       |     | 6   | 6.9                                       | 7.3  | 7.2                                      | 7.5  | 6.9                        | 7.0  | 6.9  | 6.9  | 7.1  | 7.9  |

All subjects were female Koreans (12 left femora and 12 right femora)

method is applicable even after THR, because the 3D FNC can be recognized as the volumetric center of the narrowest femoral neck prosthesis. The 3D FNC has an important meaning in that it is on the resultant load transfer line, along which load is transferred from the pelvis to the femur.

The difference between the FNAA measured by the Mod.ISS method and the 3D FNC method was 9.9° (SD = 2.7°) (Fig. 5a). On the axial plane perpendicular to the FMA, the 3D FNC method determines the FNA with the 3D FNC and the FHC. The FNAA located 7 ~ 13° anterior to that determined by the Mod.ISS method. From the proximal-most neck confluence, the anteversion angle of the FNA continuously increased distally along the FMA (Fig. 7). At L/D = 0.5 from the proximal-most neck confluence, the anteversion curve of the FNA reached to the same value of the FNAA measured by the 3D FNC method (Fig. 7). If CT images are taken almost along the FMA, one can assume that the 3D FNAA is the anteversion angle lo-

cally measured at the distal distance corresponding to half of the diameter of the femoral head (D/2) on the axial plane.

The present study has several limitations. Most importantly we did not verify FNAA using a 3D computer model or cadaveric specimens. Even though cadaveric measurements are necessary to ensure the accuracy of computer-model based measurements, the geometric error between the 3D computer models and cadaveric specimens is assumed to be less than two degrees in terms of FNAA [9, 10].

The 3D FNC method combines two gold standard methods described by Kim et al. [9] in terms of defining the FNA, and Kingsley and Olmsted's [11] in terms of defining the PFP including the PCA. The 3D FNC method for determining FNAA provides a robust and clinically accessible protocol when used with a pre-planning system such as ORTHODOC®. The authors believe that the 3D FNC method could be used as a gold standard protocol in this context. Moreover,

because it defines 3D anatomical reference points intuitively without using complex numerical calculations, the 3D FNC method can be used both pre- and post-operatively.

**Acknowledgement** This study was financially supported by Chonnam National University in 2005, and the second stage of Brain Korea 21 Program.

## References

1. Abel MF, Sutherland DH, Wenger DR, Mubarak SJ (1994) Evaluation of CT scans and 3-D reformatted images for quantitative assessment of the hip. *J Pediatr Orthop* 14(1):48–53
2. Cheng XG, Nicholson PH, Boonen S, Brys P, Lowet G, Nijs J, Dequeker J. (1997) Effects of anteversion on femoral bone mineral density and geometry measured by dual energy X-ray absorptiometry: a cadaver study. *Bone* 21(1):113–117
3. Cibulka MT (2004) Determination and significance of femoral neck anteversion. *Phys Ther* 84(6):550–558
4. Davids JR, Marshall AD, Blocker ER, Frick SL, Blackhurst DW, Skewes E (2003) Femoral anteversion in children with cerebral palsy. Assessment with two and three-dimensional computed tomography scans. *J Bone Joint Surg Am* 85(3):481–488
5. Gill HS, Alfaro-Adrian J, Alfaro-Adrian C, McLardy-Smith P, Murray DW (2002) The effect of anteversion on femoral component stability assessed by radiostereometric analysis. *J Arthroplasty* 17(8):997–1005
6. Heller MO, Bergmann G, Deuretzbacher G, Claes L, Haas NP, Duda GN (2001) Influence of femoral anteversion on proximal femoral loading: measurement and simulation in four patients. *Clin Biomech (Bristol, Avon)* 16(8):644–649
7. Hoiseth A, Reikeras O, Fonstelién E (1989) Evaluation of three methods for measurement of femoral neck anteversion. Femoral neck anteversion, definition, measuring methods and errors. *Acta Radiol* 30(1):69–73
8. Khang G, Choi K, Kim C S, Yang JS, Bae TS (2003) A study of Korean femoral geometry. *Clin Orthop Relat Res* 406:116–122
9. Kim JS, Park TS, Park SB, Kim IY, Kim SI (2000a) Measurement of femoral neck anteversion in 3D. Part1: 3D imaging method. *Med Biol Eng Comput* 38(6):603–609
10. Kim JS, Park TS, Park SB, Kim IY, Kim SI (2000b) Measurement of femoral neck anteversion in 3D. Part 2: 3D modelling method. *Med Biol Eng Comput* 38(6):610–616
11. Kingsley PC, Olmsted KL (1948) A study to determine the angle of anteversion of the neck of the femur. *J Bone Joint Surg Am* 30:745–751
12. Kuo TY, Skedros JG, Bloebaum RD (2003) Measurement of femoral anteversion by biplane radiography and computed tomography imaging: comparison with an anatomic reference. *Invest Radiol* 38(4):221–229
13. Mahaisavariya B, Sitthiseriratip K, Tongdee T, Bohez EL, Vander Sloten J, Oris P (2002) Morphological study of the proximal femur: a new method of geometrical assessment using 3-dimensional reverse engineering. *Med Eng Phys* 24(9):617–622
14. Miller F, Merlo M, Liang Y, Kupcha P, Jamison J, Harcke HT (1993) Femoral version and neck shaft angle. *J Pediatr Orthop* 13(3):382–388
15. Murphy SB, Simon SR, Kijewski PK, Wilkinson RH, Griscom NT (1987) Femoral anteversion. *J Bone Joint Surg Am* 69(8):1169–1176
16. Ruwe PA, Gage JR, Ozonoff MB, DeLuca PA (1992) Clinical determination of femoral anteversion. A comparison with established techniques. *J Bone Joint Surg Am* 74(6):820–830
17. Sugano N, Noble PC, Kamaric E (1998) A comparison of alternative methods of measuring femoral anteversion. *J Comput Assist Tomogr* 22(4):610–614
18. Tonnis D, Heinecke A (1999) Acetabular and femoral anteversion: relationship with osteoarthritis of the hip. *J Bone Joint Surg Am* 81(12):1747–1770
19. Umeda N, Saito M, Sugano N, Ohzono K, Nishii T, Sakai T, Yoshikawa H, Ikeda D, Murakami A (2003) Correlation between femoral neck version and strain on the femur after insertion of femoral prosthesis. *J Orthop Sci* 8(3):381–386
20. Yoshioka Y, Siu D, Cooke TD (1987) The anatomy and functional axes of the femur. *J Bone Joint Surg Am* 69(6):873–880